Role of nuclear densities in nucleon elastic scattering

H. F. Arellano
Department of Physics and Astronomy, University of Georgia, Athens, Georgia 30602

F. A. Brieva
Departamento de Física, Faculted de Ciencias Físicas y Matemáticas, Universidad de Chile, Casilla 487-3, Santiago, Chile
and Department of Physics and Astronomy, University of Georgia, Athens, Georgia 30602

W. G. Love
Department of Physics and Astronomy, University of Georgia, Athens, Georgia 30602
(Received 26 February 1990)

A framework based on a full-folding model of the nucleon optical potential is presented for studying nuclear densities of closed-shell nuclei using intermediate energy nucleon scattering. Using a density-matrix expansion for the mixed density, a simplified optical potential is obtained that retains the energy and momentum dependence of the effective interaction prescribed by the full-folding model. The interplay between the local density, nonlocality of the mixed-density and off-energy-shell degrees of freedom in the full-folding approach to nucleon scattering is made relatively transparent. The validity of the proposed framework is established for momentum transfers out to ~ 2.5 fm^{-1} in $p+{}^{16}$O and $p+{}^{40}$Ca scattering at energies between 200 and 400 MeV. The sensitivity of the scattering observables to nuclear densities is investigated.

I. INTRODUCTION

Recent developments[1,2] in the theory of the optical model potential for describing nucleon-nucleus elastic scattering at intermediate energies have demonstrated the importance of treating explicty the interplay between the target ground-state properties and the off-shell behavior in the nucleon-nucleon (NN) effective interaction. Indeed, by folding the fully off-shell internucleon force with the target mixed density, the full-folding model has provided a substantially improved description of elastic scattering observables for proton elastic scattering from closed-shell nuclei[2,3] at beam energies between ~ 150 and ~ 400 MeV. However, the complexity of the full-folding approach makes it difficult to distinguish the primary role of the target density from that of the effective force. In fact, recent implementations of the full-folding optical potential make use of single-particle models to represent the target ground state, thus relying on single-particle wave functions rather than on more global properties such as the matter distributions.

In this paper we address the question of how the full-folding optical potential may provide useful information about ground-state nucleon densities from intermediate energy elastic scattering. Since the effective internucleon force can be assumed to be relatively well defined over the energy range considered here, we investigate the possibility of using an approximation to the exact full-folding calculation in which the target densities are clearly identified. Our present approach is based on expansions of the target mixed density[4,5] and leads to a more transparent formulation of the optical potential while retaining the dominant features peculiar to the full-folding model. Physically, we expect to gain insight as to how the nonlocality of the mixed density samples the relevant energies and off-shell components of the effective force. Furthermore, it becomes possible to connect the nucleon optical potential to measured rather than model matter distributions within the range of validity of the approximate full-folding scheme.

There are alternative approximations to the full-folding model which make explicit the dependence of the optical potential on the density.[1,6,7] The best known approximation leads to the standard $t\rho$ model which is essentially based on assumptions about the Fermi motion of the struck nucleon in the target thus simplifying the off-shell components of the effective force that enter in the optical potential calculation. Although attractive in its formal structure, the $t\rho$ model is a poor approximation to the full-folding model below ~ 400 MeV.[3,6] In particular it fails to explain the scattering observables at these energies especially at small momentum transfers.

The assumptions involved in the present approach differ from those in the $t\rho$ model in the sense that, by approximating the mixed density, we still account for most of the relevant aspects of the Fermi motion of the nucleons in the target and therefore need the full off-shell interaction. The weak sensitivity of the full-folding calculation to the details of this approximation indicates that nucleon elastic scattering may be used for extracting direct information about the matter distribution of the target.

This paper is developed as follows: In Sec. II we derive a simplified expression for the full-folding optical potential for intermediate-energy elastic proton scattering based on the local-density (Slater) and Campi-Bouyssy approximations[4] to the target mixed density in a momentum-space representation. In Sec. III we present our results. We discuss the properties of the approximate mixed density and assess the validity of the full-folding

optical potential in this context. We also study the sensitivity of the scattering observables to the matter distributions by comparing the results obtained from measured and modeled densities. In Sec. IV we present our conclusions.

II. MIXED DENSITIES AND THE NUCLEON-NUCLEUS OPTICAL POTENTIAL

The microscopic description of nucleon elastic scattering from nuclei requires the calculation of the nucleon-nucleus optical potential. Since off-energy-shell degrees of freedom of the internucleon force are most easily identified in momentum space, we use this representation to describe the full-folding optical potential and to obtain an approximation to it.

Following the Watson[8] and Kerman, McManus, and Thaler[9] theories for nucleon-nucleus elastic scattering, assuming a single-particle description for the target ground state, and neglecting recoil effects and medium corrections, the optical potential is given by[2]

$$U(\mathbf{k}',\mathbf{k};E)=\sum_{\alpha}\int d\mathbf{Q}\,\varphi_{\alpha}^{\dagger}(\mathbf{Q}-\mathbf{k}')\left\langle \mathbf{k}'-\tfrac{1}{2}\mathbf{Q}\left|\hat{t}\left[E+\varepsilon_{\alpha}-\frac{Q^2}{2M}\right]\right|\mathbf{k}-\tfrac{1}{2}\mathbf{Q}\right\rangle_{\mathcal{A}}\varphi_{\alpha}(\mathbf{Q}-\mathbf{k})\ , \tag{1}$$

where φ_α are the occupied single-particle states of energy ε_α, E is the projectile kinetic energy, M is the total mass of the interacting pair, and $\mathbf{Q}$ is their total momentum. The free NN t matrix $\hat{t}(\omega)$ is calculated from the bare internucleon potential v by solving the Lippmann-Schwinger integral equation

$$\hat{t}(\omega)=v+v\frac{1}{\omega-K+i\eta}\hat{t}(\omega)\ , \tag{2}$$

where K represents the kinetic energy operator for the relative motion. We note that for calculating the optical potential given by Eq. (1) the effective interaction should be evaluated at energies which depend on each single-particle energy ε_α. If the energy variation of the t matrix is strong enough to make the ε_α variation important, the full folding has to be performed as indicated in Eq. (1) and no reference to the target density can be simply obtained. However, as the projectile energy E increases, the variation of ε_α becomes relatively unimportant. Indeed, for nucleon scattering above $\sim$100 MeV it should be reasonable to replace the ε_α by $\langle\varepsilon\rangle$, the weighted energy average of the occupied target single-particle states. With this replacement and after summing over the struck-nucleon spin states, Eq. (1) for the optical potential becomes

$$U(\mathbf{k}',\mathbf{k};E)=\int d\mathbf{Q}\,\rho(\mathbf{Q}-\mathbf{k}',\mathbf{Q}-\mathbf{k})\times\hat{t}\left[\mathbf{k}'-\tfrac{1}{2}\mathbf{Q},\mathbf{k}-\tfrac{1}{2}\mathbf{Q};E+\langle\varepsilon\rangle-\frac{Q^2}{2M}\right]\ , \tag{3}$$

with

$$\rho(\mathbf{p}',\mathbf{p})=\sum_{\alpha}\varphi_{\alpha}^{\dagger}(\mathbf{p}')\varphi_{\alpha}(\mathbf{p})\ , \tag{4}$$

and

$$\hat{t}(\boldsymbol{\kappa}',\boldsymbol{\kappa};z)=\langle\boldsymbol{\kappa}'|\hat{t}(z)|\boldsymbol{\kappa}\rangle_{\mathcal{A}}\ . \tag{5}$$

Thus Eq. (3) is an expression for the full-folding optical potential in which the target mixed density ρ appears explicitly. This is the starting point for developing an approach to investigate the role of different aspects of $\rho(\mathbf{p}',\mathbf{p})$ in the full-folding model and for studying the sensitivity of the scattering observables to them.

At this point it is convenient to define the following set of variables:

$$\mathbf{q}=\mathbf{k}-\mathbf{k}',\quad \mathbf{K}=\tfrac{1}{2}(\mathbf{k}+\mathbf{k}'),\quad \mathbf{P}=\mathbf{Q}-\mathbf{K}=\tfrac{1}{2}(\mathbf{p}+\mathbf{p}')\ . \tag{6}$$

These definitions lead to the following expression for the optical potential

$$U(\mathbf{k}',\mathbf{k};E)=\int d\mathbf{P}\,\rho(\mathbf{P}+\tfrac{1}{2}\mathbf{q},\mathbf{P}-\tfrac{1}{2}\mathbf{q})\hat{t}(\boldsymbol{\kappa}',\boldsymbol{\kappa};z)\ , \tag{7}$$

where we have denoted

$$\boldsymbol{\kappa}'=\tfrac{1}{2}(\mathbf{K}-\mathbf{P}-\mathbf{q}),\quad \boldsymbol{\kappa}=\tfrac{1}{2}(\mathbf{K}-\mathbf{P}+\mathbf{q})\ ,$$
$$z=E+\langle\varepsilon\rangle-\frac{(\mathbf{P}+\mathbf{K})^2}{2M}\ . \tag{8}$$

For actual calculations, Eq. (7) for the optical potential separates into proton and neutron contributions in the form $U\sim\rho_p\hat{t}_{pp}+\rho_n\hat{t}_{pn}$. To simplify the notation, the symbol ρ and associated quantities will refer to protons *or* neutrons without distinction. The same consideration holds for the t matrix.

The mixed-density in a momentum representation can be simply related to its coordinate representation $\rho(\mathbf{r}',\mathbf{r})$ by a Fourier transformation. In terms of the full-folding variables this relationship is given by

$$\rho(\mathbf{P}+\tfrac{1}{2}\mathbf{q},\mathbf{P}-\tfrac{1}{2}\mathbf{q})=\frac{1}{(2\pi)^3}\int d\mathbf{R}\,d\mathbf{r}\,e^{i\mathbf{R}\cdot\mathbf{q}}e^{i\mathbf{r}\cdot\mathbf{P}}\rho(\mathbf{R}+\tfrac{1}{2}\mathbf{r},\mathbf{R}-\tfrac{1}{2}\mathbf{r})\ . \tag{9}$$

Campi and Bouyssy[4] (CB) have shown that to a very good approximation, the single-particle mixed density in coordinate space for protons and neutrons can be cast in the Slater form

$$\rho(\mathbf{R}+\tfrac{1}{2}\mathbf{r},\mathbf{R}-\tfrac{1}{2}\mathbf{r})\simeq\rho(R)F(R;r)\ . \tag{10}$$

In this approximation, $\rho(R)$ is the usual nuclear point density given by the diagonal terms of the general mixed density and $F(R;r)$ is a measure of the nonlocality of the mixed density. In order to ensure that the matter form

factor is correctly reproduced, the condition $F(R;0)=1$ must be satisfied.

The most appealing feature of the approximate mixed-density given by Eq. (10) is the absence of any dependence on the angle between **R** and **r**. The reliability of this approximation in the context of nucleon-nucleus scattering needs to be established through calculations of scattering observables from fully-folded optical potentials using the exact and approximate mixed densities. We shall address this point in the following section, where we examine the validity of this approximation for a particular choice of $F(R;r)$.

Following CB, we have assumed for $F(R;r)$ the structure suggested by nuclear matter, namely

$$F(R;r)=3\frac{j_1(\hat{k}(R)r)}{\hat{k}(R)r} , \tag{11}$$

where j_1 is the spherical Bessel function of order 1. The choice of $\hat{k}(R)$ depends on the level of approximation we require for the mixed density. The simplest choice corresponds to the Slater form,

$$\hat{k}_S(R)=[3\pi^2\rho(R)]^{1/3} , \tag{12}$$

while a more accurate expansion for the mixed density leads to the CB choice,[4]

$$\hat{k}_{\rm CB}(R)=\left\{\frac{5}{3\rho(R)}[\tau(R)-\tfrac{1}{4}\nabla^2\rho(R)]\right\}^{1/2} ; \tag{13a}$$

with

$$\tau(R)=\sum_\alpha |\nabla\varphi_\alpha(\mathbf{R})|^2 . \tag{13b}$$

The subject of investigating alternative forms for $F(R;r)$ remains open. As we will see, this function is important in that it determines the extent to which the momentum dependence of the t matrix is operative in the full-folding model framework of the optical potential.

Using the approximation for the mixed density given by Eq. (10), the following result is obtained for its momentum space representation [Eq. (9)],

$$\rho(\mathbf{P}+\tfrac{1}{2}\mathbf{q},\mathbf{P}-\tfrac{1}{2}\mathbf{q})\approx\rho(q;P) , \tag{14}$$

with

$$\rho(q;P)=\frac{1}{(2\pi)^3}\int d\mathbf{R}\, e^{i\mathbf{R}\cdot\mathbf{q}}\rho(R)G(R;P) , \tag{15a}$$

where, from Eqs. (9) and (10),

$$G(R;P)=\int d\mathbf{r}\, e^{i\mathbf{r}\cdot\mathbf{P}}F(R;r) . \tag{15b}$$

For the functional form of $F(R;r)$ given by Eq. (11), it is straightforward to show that

$$G(R;P)=\frac{2}{\hat{\rho}(R)}\Theta[\hat{k}(R)-P] , \tag{16}$$

where $\hat{\rho}(R)$ is analogous to the local nuclear matter density and is given by

$$\hat{\rho}(R)=\frac{\hat{k}(R)^3}{3\pi^2} . \tag{17}$$

It is clear from Eqs. (12) and (17) that in the infinite nuclear matter limit, the Slater form, we have $\hat{\rho}(R)=\rho(R)$.

The present scheme for calculating the mixed density has the significant practical advantage that matter (or at least proton) distributions $[\rho(R)]$ obtained from elastic scattering rather than from models can be used "directly." Although the function $G(R,P)$ has been constructed on the basis of single-particle models, this function may be parametrized to study effects absent in such a description of the target ground state. For the choice of $F(R;r)$ suggested by nuclear matter and given by Eq. (11), the mixed density in momentum space takes the form

$$\rho(q;P)=\frac{2}{(2\pi)^3}\left\{4\pi\int_0^\infty R^2dR\frac{\rho(R)}{\hat{\rho}(R)}j_0(qR)\times\Theta[\hat{k}(R)-P]\right\} . \tag{18}$$

With the use of Eq. (7) for the nucleon-nucleus optical potential and Eq. (14) for the mixed density one obtains

$$U(\mathbf{k}',\mathbf{k};E)=\int d\mathbf{P}\,\rho(q;P)\hat{t}(\boldsymbol{\kappa}',\boldsymbol{\kappa};z) , \tag{19}$$

with $\rho(q;P)$ given by Eq. (15). In the Slater and CB approximations this function vanishes for all values of P above $\hat{k}_{\rm max}$, the maximum $\hat{k}(R)$ allowed, thus determining the admissible values of **P** and the sampling of off-shell degrees of freedom [see Eq. (8)]. This feature can be made explicit when using the Slater approximation. Indeed, if we assume a continuously decreasing function for the density $\rho(R)$ and therefore for $\hat{k}_S(R)$, the mixed density $\rho(q;P)$ can be evaluated directly. We obtain

$$\rho_S(q;P)=\frac{2}{(2\pi)^3}[\tfrac{4}{3}\pi R^3_{\rm max}(P)]\times S[qR_{\rm max}(P)]\Theta(\hat{k}_{\rm max}-P) , \tag{20}$$

where $R_{\rm max}$ is calculated from $\hat{k}_S(R_{\rm max})=P$ for each P less than $\hat{k}_{\rm max}$ and $S(x)=3j_1(x)/x$ is the usual Slater function. Equation (20) has a simple interpretation. The volume within $R_{\rm max}$ is that volume of the nucleus which supports momenta P [Eq. (6)]; the factor of 2 corresponds to the assumed spin degeneracy. The Slater function (which peaks at $q=0$) determines the relative probability with which the nucleus can support a given momentum transfer and the step function restricts the momentum P to its allowed domain. For $P\lesssim\hat{k}_{\rm max}$, $R_{\rm max}$ is relatively small (see Fig. 2) leading to comparable probabilities for transferring large and small momenta. Conversely, when P is small, $R_{\rm max}$ is relatively large and large momentum transfers are inhibited. For the CB approximation, an analytic result cannot be obtained. However, the general trend indicated by Eq. (20) remains.

Equation (19) has the folding structure of the optical potential in terms of the nuclear mixed density and the effective interaction. The prescription for averaging the effective interaction takes into consideration the local momentum $\hat{k}(R)$ and requires explicit off-shell contributions of the NN effective interaction determined by the Fermi motion of the struck nucleon. The interplay between off-shell degrees of freedom and the nonlocality of

the target ground-state mixed density is explicit. This interplay is characteristic of the full-folding model and is often neglected in alternative approaches. In fact, if we assume that the t matrix does not vary significantly in the range of variation of $\mathbf{P}$, the full-folding optical potential reduces to the $t\rho$ structure

$$U_{t\rho}(\mathbf{k}',\mathbf{k};E)=\rho(q)\hat{t}(\kappa',\kappa;z)|_{\mathbf{P}\approx 0}\ , \tag{21}$$

and no information on the nonlocality of the mixed density, the F function, is obtained even though the off-shell t-matrix enters, albeit over a restricted range in momentum space. Equation (21) is the "off-shell $t\rho$" approximation introduced in Ref. 10 and applied in Refs. 1, 3, and 7.

III. RESULTS

In this section we examine the validity of the approximated mixed density in calculations of the full-folding optical potential for intermediate energy proton elastic scattering. The NN effective interaction used throughout is the free t matrix obtained by solving Eq. (2) using the Paris potential.[11] No approximations were made to treat the momentum and energy dependence of the t matrix on or off the energy-shell.

A. The mixed density

We have calculated the exact mixed density for a single-particle model generated by a Woods-Saxon (WS) potential adjusted for each state in order to obtain a good fit to the single-particle energies, the rms radius, and the charge form factor. Using the same single-particle wave functions we have calculated the approximate $\rho(q;P)$ expressed in Eqs. (14)–(16) for both Slater and CB prescriptions. In order to gauge the validity of these approximations, we have considered the ^{40}Ca nucleus and show in Fig. 1 plots of the quantity $P^2\rho(+\frac{1}{2}\mathbf{q},\mathbf{P}-\frac{1}{2}\mathbf{q})$ using the exact [Fig. 1(a)] and approximate expressions, CB [Fig. 1(b)] and Slater [Fig. 1(c)], for the mixed density. In the case of the exact mixed density we have taken the angle between $\mathbf{q}$ and $\mathbf{P}$ to be zero. Alternative choices for the angle between $\mathbf{q}$ and $\mathbf{P}$ lead to figures which are indistinguishable from Fig. 1(a). This observation is consistent with the CB approximation, in which the mixed density does not depend on the angle between $\mathbf{r}$ and $\mathbf{R}$. The overall features of the exact density are similar to those given by the approximate ones with the exception of the asymptotic behavior in the P coordinate (the mean bound-state momentum). The approximate mixed density shows clearly the allowed range of integration for the full-folding calculation as well as where the relative weight of the density is greater in terms of sampling the off-shell effects.

The differences in Figs. 1(b) and 1(c) reflect different treatments for the nonlocality of the mixed density. Although the CB and Slater approximations each use form factors for the nonlocality given by Eq. (11), they differ in their choice of $\hat{k}(R)$. In Fig. 2 we have plotted the proton density for ^{40}Ca obtained from the WS single-particle model and the calculated $\hat{k}(R)$ in the two approximations considered. It is clear that for $R \lesssim 4$ fm both choices of $\hat{k}(R)$ yield similar values and that the largest differences occur near the nuclear surface. Also, both approximations yield a similar maximum value for $\hat{k}(R)$ (~ 1.3 fm^{-1}) thus explaining the similar behavior of the mixed density as a function of P in Fig. 1. Results similar to those shown in Figs. 1 and 2 have been found for ^{16}O. We conclude that the Slater and CB approximations differ mainly in their treatment of the nuclear surface. This result is reflected in slightly different matter distributions in momentum space as shown in Fig. 1.

The question as to whether we can discriminate between the Slater and CB approximations from intermediate energy elastic nucleon scattering, and therefore learn detailed aspects about the nonlocality of the mixed density, will be addressed in the next section.

B. Approximate full-folding optical potential

To test the reliability of the approximate mixed densities within the full-folding framework we have calculated optical potentials and the associated elastic scattering observables using Eqs. (3) and (19). We have studied the

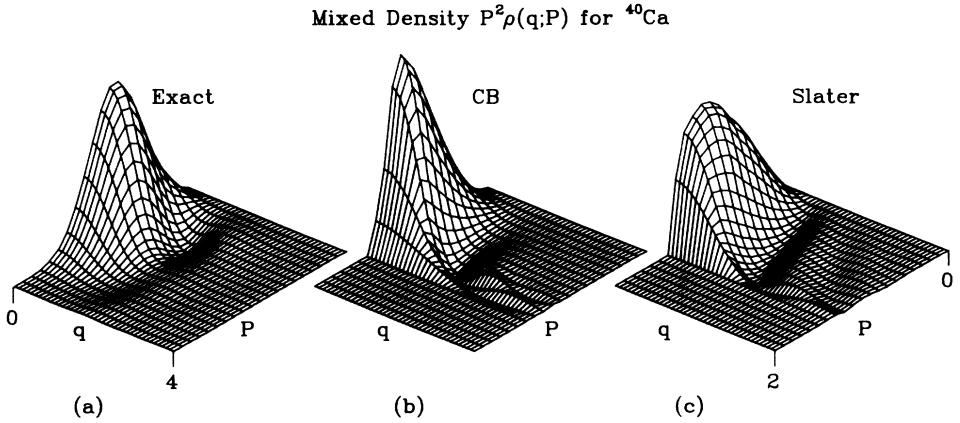

FIG. 1. Mixed densities for ^{40}Ca in a momentum space representation: (a) corresponds to a WS model with the angle between $\mathbf{q}$ and $\mathbf{P}$ set equal to zero; (b) Campi-Bouyssy approximation, and (c) Slater approximation. The momenta are in fm^{-1}.

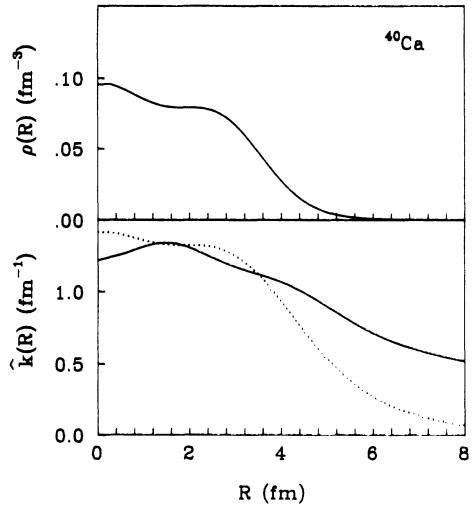

FIG. 2. Proton density for ^{40}Ca from a WS model and CB (solid curve) and Slater (dotted curve) approximations for $\hat{k}(R)$—Eqs. (13) and (12), respectively.

200–400 MeV energy range for proton elastic scattering from ^{16}O and ^{40}Ca where the full-folding model has proved to be quite successful in reproducing the data.[2,3] In Fig. 3 we present the calculated cross sections ($d\sigma/d\Omega$), analyzing powers (A_y) and spin rotation parameters (Q) for $p+^{16}$O elastic scattering at 200 MeV and $p+^{40}$Ca elastic scattering at 400 MeV. Solid curves

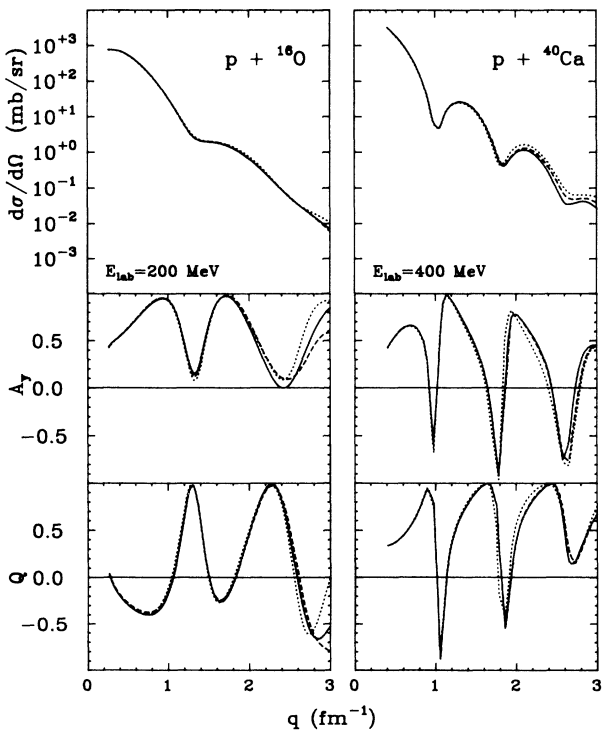

FIG. 3. Scattering observables for $p+^{16}$O at 200 MeV and $p+^{40}$Ca at 400 MeV from full-folding model calculations using the exact mixed density (solid curves) and its CB (dashed curves) and Slater (dotted curves) approximations.

represent results obtained using the exact mixed density; the dashed curves represent results using the CB approximation and the dotted curves correspond to the Slater approximation. We observe that the calculated observables using the exact and approximate mixed densities are remarkably similar for momentum transfers below ~ 2 fm^{-1}, a region in which the importance of off-shell effects has been demonstrated.[3] For q between ~ 2.0 and 2.6 fm^{-1} the approximate calculations begin to deteriorate, with the CB approximation following the results based on the exact mixed density more closely than does the Slater approximation. For $q \gtrsim 2.6$ fm^{-1} neither approximation is satisfactory for all the observables, especially for the smaller ^{16}O target. Similar results are obtained for proton scattering on ^{40}Ca and ^{16}O at other energies within the range considered here.

Although both approximations to the mixed density are quite good for calculating the full-folding optical potential, the CB approximation is observed to be slightly superior. This result is consistent with the better treatment of the nuclear surface provided by the CB approximation. In fact, we have investigated this point and found that the full-folding results are equally well reproduced for momentum transfers in the range 0–2.5 fm^{-1} if we use a $\hat{k}_{\rm CB}$ constructed from a harmonic oscillator model. However, we can still use the Slater approximation below $q \approx 2.5$ fm^{-1} to get a good estimate of the scattering observables. This has the important practical advantage of being able to express the optical potential in terms of conventional nuclear densities and the off-shell t matrix. No further model is required to obtain $\hat{k}_S(R)$ other than the trivial nuclear matter relationship [Eq. (12)] between $\hat{k}_S$ and the nuclear density.

The results in Fig. 3 also indicate that proton scattering at these intermediate energies is not especially sensitive to the detailed form of the nonlocality in the mixed density. Indeed, the different mixed densities in Fig. 1 provide very similar samplings of the momentum dependence of the effective force; the differences only slightly affect the scattering observables shown in Fig. 3, mainly for $q \gtrsim 2.5$ fm^{-1}.

C. Sensitivity to the density

Since it has been shown that a full-folding calculation can be simplified so as to be expressed in terms of the nuclear matter density, $\hat{k}(R)$, and the off-shell effective force, we can now test directly the sensitivity[12] of the optical potential and the corresponding scattering observables to the densities.

From the results in Fig. 3 we can assume that the observables calculated from the CB approximation correspond to the exact results, especially for $q \lesssim 2.5$ fm^{-1}. Therefore, we have performed calculations of full-folding optical model potentials for $p+^{40}$Ca scattering at 200 MeV using the CB approximation and three different proton densities with the same rms radius. One of them was determined from electron scattering,[13] and the other two were calculated from a WS and a harmonic oscillator (HO) model, respectively. In all cases the neutron densities were assumed to be equal to the proton ones. The nonlocality function $\hat{k}_{\rm CB}$ was obtained from the WS

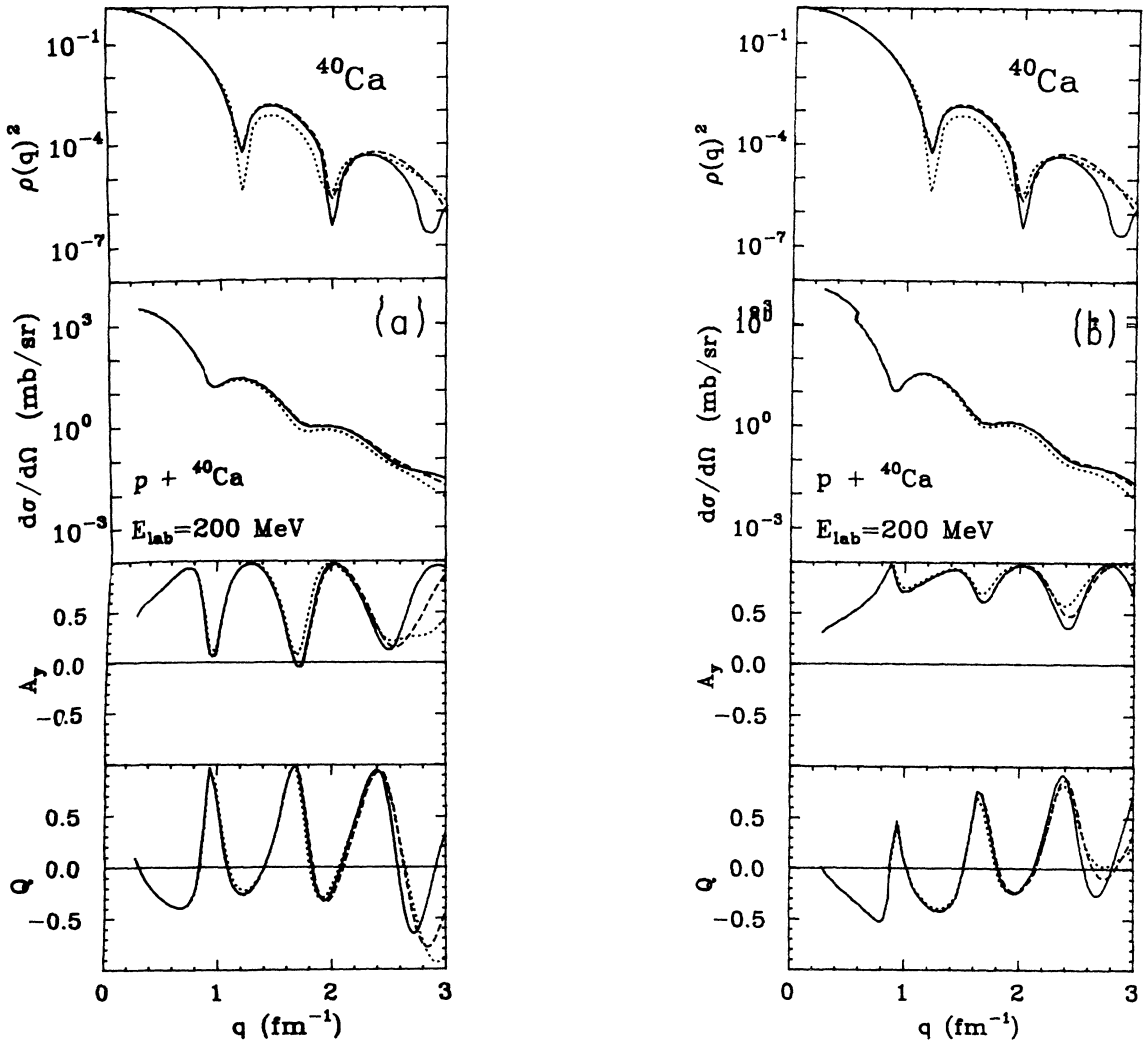

FIG. 4. (a) Sensitivity of scattering observables to the density in the full-folding framework. The upper frame shows the squared-Fourier transform of the phenomenological (solid curve), WS model (dashed curve), and HO model (dotted curve) densities. Scattering observables are calculated using the same $\hat{k}_{CB}$ for the phenomenological (solid curves), WS (dashed curves) and HO (dotted curves) densities. (b) Sensitivity of the scattering observables to the density in the local $t\rho$ approximation. Solid, dashed, and dotted curves denote results obtained using the phenomenological, WS, and HO densities, respectively.

single-particle model. In the upper frame of Fig. 4(a) we show the squared Fourier transform of the point proton densities. The solid curve represents the density based on a phenomenological charge density.[13] The dashed and dotted curves are used to represent the point proton density from WS and HO single-particle models, respectively. In Fig. 4(a) we also plot the scattering observables as a function of the momentum transfer obtained from full-folding calculations using the approximate scheme for the mixed density. Solid curves correspond to the phenomenological local density, and dashed and dotted curves to the WS and HO models, respectively. We observe that the form factors for the phenomenological density and WS model differ only in the $q \approx 2-3$ fm^{-1} region, whereas differences of the HO model relative to the phenomenological density occur between ~ 1 and ~ 2 fm^{-1}. In the case of the calculated scattering observables, the major differences are observed between the phenomenological and HO densities. These differences are most pronounced in the cross section; the spin observables show less sensitivity to the densities, except for $q \gtrsim 2.5$ fm^{-1}. Considering that all the calculations were made with the same nonlocality factor and corresponding $\hat{k}_{CB}$ in the mixed density, the differences found in the scattering observables are a direct measure of the differences in the densities. In order to illustrate the relative *sensitivity* of the scattering observables to the nuclear density within different frameworks, we show in Fig. 4(b) results of analogous calculations using the local "$t\rho$" approximation for the optical potential. The level of sensitivity of the calculated results to the nuclear density using the two models is found to be comparable. However, the present approximate version of the full-folding model enables one to treat the energy and momentum dependence of the NN t matrix in a much more accurate way, which leads to more confidence in the extracted information on the nu-

clear density. The point is that where reliable NN potentials are available, only a minimal amount of very weakly model-dependent information $[\hat{k}(R)]$ needs to be introduced in order to study the nuclear density within the present framework. A detailed study of matter densities from proton scattering data is beyond the scope of the present work.

IV. CONCLUSIONS

We have presented a framework for studying and interpreting the role of target densities in nucleon-nucleus scattering at intermediate energies. The approach is based on an approximation to the mixed density in the full-folding model. The advantage of this approximation is that it retains the essential features of the exact approach while providing a simple functional form for the optical potential in terms of the nuclear matter distributions and the nonlocality of the mixed density. The validity of the approximate scheme has been verified by performing calculations of the full-folding optical potential for $p+{}^{16}\mathrm{O}$ and $p+{}^{40}\mathrm{Ca}$ at energies between 200 and 400 MeV and by comparing the elastic scattering observables with those obtained using exact procedures. The approximate framework is very reliable out to $q\sim 2$ fm^{-1} and reasonable out to $q\sim 2.6$ fm^{-1}.

We have shown that there is little sensitivity in the scattering observables to small differences in the nonlocality of the mixed-density. This leads to a mixed density model for the nucleon optical potential, which is simpler to calculate, and, more importantly, depends on measured rather than modeled densities to describe the target nucleus. Although the best (CB) approximation to the mixed density is model dependent through the determination of $\hat{k}$, this model dependence is relatively weak, especially when $\hat{k}$ is generated from a single-particle model with a size characteristic of the nucleus being studied. For $q\lesssim 2$ fm^{-1} the Slater approximation for $\hat{k}$ is adequate.

The simplicity of the present model enables us to better understand the overall role of target ground-state densities in intermediate energy nucleon scattering and represents a natural extension of earlier techniques based on a local $t\rho$ scheme.[12] Alternatively, considering the sensitivity of the full-folding model to the matter density, nucleon scattering data may be used to complement accurate determinations of proton densities from electron scattering and to determine properties of neutron densities.

ACKNOWLEDGMENTS

This work was supported in part by the National Science Foundation, Grant Nos. PHY-8607684 and PHY-8903856. F.A.B. acknowledges partial support from the Fondo Nacional de Desarrollo Científico y Tecnológico, Chile, Grant No. 1212-88. We also appreciate a grant for computing time provided by the University Computing and Networking Services of the University of Georgia.

[1]Ch. Elster, Taksu Cheon, Edward Redish, and P. C. Tandy, Phys. Rev. C **41**, 814 (1990).
[2]H. F. Arellano, F. A. Brieva, and W. G. Love, Phys. Rev. Lett. **63**, 605 (1989).
[3]H. F. Arellano, F. A. Brieva, and W. G. Love, Phys. Rev. C **41**, 2188 (1990).
[4]X. Campi and A. Bouyssy, Phys. Lett. **73B**, 263 (1978).
[5]J. W. Negele and D. Vautherin, Phys. Rev. C **5**, 1472 (1972).
[6]L. Ray and G. W. Hoffmann, Phys. Rev. C **31**, 538 (1985).
[7]Ch. Elster and P. C. Tandy, Phys. Rev. C **40**, 881 (1989).
[8]K. M. Watson, Phys. Rev. **89**, 575 (1953); A. L. Fetter and K. M. Watson, in *Advances in Theoretical Physics*, edited by K. A. Brueckner (Academic, New York, 1965), Vol. 1.
[9]A. K. Kerman, H. McManus, and R. M. Thaler, Ann. Phys. (N.Y.) **8**, 551 (1959).
[10]A. Picklesimer, P. C. Tandy, R. M. Thaler, and D. H. Wolfe, Phys. Rev. C **30**, 1861 (1984).
[11]M. Lacombe, B. Loiseau, J. M. Richard, R. Vinh Mau, J. Côté, P. Pirès, and R. de Tourreil, Phys. Rev. C **21**, 861 (1980).
[12]L. Ray and G. W. Hoffmann, Phys. Rev. C **27**, 2143 (1983); L. Ray, *ibid.* **19**, 1855 (1979).
[13]B. B. P. Sinha, G. A. Peterson, R. R. Whitney, I. Sick, and J. S. McCarthy, Phys. Rev. C **7**, 1930 (1973).